RSC Advances

ROYAL SOCIETY OF CHEMISTRY

www.rsc.org/advances

Journal Name

ARTICLE

PET governed fluorescence "Turn ON" BODIPY probe for selective detection of picric acid.

Received 00th January 20xx,
Accepted 00th January 20xx

DOI: 10.1039/x0xx00000x
www.rsc.org/

Yogesh Erande, Santosh Chemate, Ankush More and Nagaiyan Sekar*

The non fluorescent meso diaminophenyl 1, 3, 5, 7-tetramethyl BODIPY dye has been investigated and employed for picric acid sensing in constructive way by regenerating its fluorescence through PET hindrance. Strong enhanced emission signal was obtained as consequence of electrostatic association between BODIPY probe and picric acid with specific recognition among other explosive nitro aromatics. The probe shows 1:1 binding stoichiometry with picric acid and detection limit up to 0.65ppb.

Introduction

Now a day's danger of terrorism with increased use of high explosives challenges the modern technology for their detection and screening[1]. Electron deficient nitro aromatics (NACs)are preferred explosives and picric acid(PA) is one of them whose explosive power is equivalent to 105% of trinitrotoluene(TNT) known as primary explosives[2,3]. PA is an important chemical and finds applications in medicinal formulations in the treatment of malaria, trichinosis, herpes, smallpox, and antiseptics[4], in dye industries and chemical laboratories[5,6], in the manufacture of rocket fuels, fireworks, sensitizers in photographic emulsions, as a component in matches[7–9]. Owing to its electron-deficient character the degradation of PA in bio system is difficult making it as an environmental contaminant[10]. As an effect of nitro and phenol functionalities, PA causes strong irritation to the skin, eye and potential damage to organs of respiratory system[8,9]. Therefore rapid, cheap, sensitive and selective detection of picric acid is of prime importance. Various analytical techniques such as gas chromatography, ion mobility spectrometry, Raman spectroscopy, and fluorescence spectroscopy have been reported for the detection of NACs explosives[11]. Further, among various techniques adopted for detection of NACs, fluorescence signalling is superior with high sensitivity, specificity, real-time monitoring with short response time and easy sample preparation[12] while other methods cannot be used in the field due to their high cost, lack of selectivity and sensitivity[13]. Analyte sensing by fluorescent probe after binding with it is attributed to either enhancement or quenching of fluorescence[14,15]. Stoichiometric binding over collisional phenomenon and less interference from fluctuation of background fluorescence make fluorescence enhancement method more preferable than quenching of fluorescence for analyte sensing[16,17]. Metal–organic framework [18–22] and organic or inorganic conjugated polymers [23,24], are mostly employed as fluorescent sensors for the detection of poly nitro aromatics particularly picric acid. In the field of NACs detection application of metal organic framework, quantum dots mostly contain cadmium and pyrene class of sensors are challenged by their toxicity[18,21,25,26]. Among the available sensors for picric acid detection by quenching of fluorescence [18,27–31] are more explored than 'no quenching fluorescence sensors' [32–36]. In the current scenario p-terphenylbenzimidazolium-based molecular baskets [37], zinc-phthalocyanine framework based chemosensor with fluorescence quenching [38,39], electron-rich triphenylamine-based sensors with charge-transfer complex formation[40], electrogenerated thin films of microporous polymer networks-response to NACs[41], glucopyranosyl-1,4-dihydropyridine chemosensor[42], metal–organic framework $[Cd_3(TPT)_2(DMF)_2]\cdot(H_2O)_{0.5}$ for NACs detection[43], self-assembled nanoscopic organic cage for PA detection[44] are some strategies focusing on NACs explosive detection. Most of above the discussed molecules or strategies are complicated so small molecules as fluorescence sensor having better option as they are easy to synthesize and their properties can be easily tuned by structural modifications for desired sensing specificity. BODIPY dyes are versatile fluorescent probes comprising various properties such as high chemical and photo stability , high absorption coefficients and sharp fluorescence peaks with high quantum yields[45,46]. With number of possible structural modifications it is easy to design the BODIPY luminophore for desired spectroscopic and photophysical

Tinctorial Chemistry Group, Department of Dyestuff Technology, Institute of Chemical Technology, Mumbai-400 019, India.
E-mail: n.sekar@ictmumbai.edu.in; nethi.sekar@gmail.com;
Tel: +91 22 3361 2707

characteristics as chemosensor[45–50]. Some sensors with aromatic amine showed selectivity and sensitivity for picric acid but they are synthetically challenging [22,51]. Considering the entire dilemma we have presented the current BODIPY probe as selective turn on fluorescent chemosensor for picric acid detection among other NACs. This molecule possesses very weak fluorescence which gets enhanced as consequence of inhibition of photoinduced electron transfer (PET) phenomenon. Perpendicular meso diaminophenyl moiety quenches the emission from BODIPY core through PET utilising its lone pairs which are now associated with PA by static interaction so to leave BODIPY core to fluoresce that demonstrate the fluorescence turn on PA sensing.

Experimental

Fluorescence spectra were recorded on a Varian Carry Ecllips Spectrofluorometer. UV/Visible spectra were recorded on a Perkin Elmer Lambda-25 spectrophotometer using a 10 mm path length quartz cell. The photophysical study was carried out in HPLC-grade solvents. NMR spectra were recorded in DMSO-d_6 solution on the Agilent-500 MHz instruments, and the chemical shifts are reported in δ values (ppm) relative to TMS. 3, 5-dinitro benzoyl chloride was purchased from Sigma Aldrich. All solvents used for synthesis were of synthetic grade and purchased from s d Fine Chemicals, India. Other chemicals/ reagents were purchased from commercial sources. The reactions were carried out under nitrogen atmosphere and dichloromethane was dried by treatment with calcium hydride before use.

Determination of apparent association constants (Ka) of PA binding with sensor

The binding constant was calculated from the emission intensity-titration plot of 1/ (I-Io) as a function of 1/ [PA] in mole. Io and I are the fluorescence intensities of BODIPY-2 without and with added PA. BODIPY-2 with a concentration of 1 × 10 −6mol/L in absolute ethanol was used for the fluorescence titration studies with a PA. The PA concentration was varied from 4 to 13 eq. for this titration. The apparent binding constant for the formation of the complex was evaluated using the Benesi–Hildebrand plot.

Estimation of detection limit

Fluorescence titration of probe (conc. =1 × 10^{-6}mol/L) with PA in ethanol was carried out by adding aliquots of PA from 1 to 12 equivalents. Standard deviation (SD) was obtained from 10 blank reading of probe (conc. =1 × 10^{-6}mol/L). From the plot of fluorescence intensity as a function of the added PA eq., the slope was obtained. Then the detection limit (DL) was calculated from equation DL= (3xSD)/slope.

Determination of the binding stoichiometry

Stoichiometry of probe-analyte was determined by continuous variation method known as Job's plot. In this experiment total concentration of probe and analyte ([BODIPY] + [PA]) was kept constant (30μM) and the ratio was varied for 10 different fractions. The Job's plot was obtained by plotting fluorescence intensity (I-Io) as a function of mole fraction of PA.

Computational method

All DFT computations were performed using the Gaussian09 (G09) program[52,53]. Full geometry optimization of BODIPY-2 and its complex with PA were carried out using the hybrid functional B3LYP and the Pople's double zeta basis set 6-31G(d)[54,55].

Synthesis of BODIPY-1 and 2

2, 4 Dimethyl pyrrole was prepared by the reported method [56]**.** BODIPY-1 and BODIPY-2 was synthesized with gentle modifications in reported procedure [57]. BODIPY-1 &2 were characterised by ^{1}H and ^{13}C NMR.

BODIPY-1: ^{1}H NMR (500 MHz, cdcl$_3$) δ (ppm)
9.19 (t, *J* = 2.1 Hz, 1H), 8.59 (d, *J* = 2.1 Hz, 2H), 6.07 (s, 2H), 2.59 (s, 6H), 1.37 (s, 6H).
BODIPY-1: ^{13}C NMR (126 MHz, cdcl$_3$) δ (ppm)
158.00, 149.01, 141.78, 138.81, 134.50, 130.67, 129.13, 122.59, 119.34, 15.38, 14.75.
BODIPY-2: ^{1}H NMR (500 MHz, DMSO-d_6) δ (ppm)
6.13 (s, 2H), 5.90 (t, *J* = 2 Hz, 1H), 5.67 (d, *J* = 2.0 Hz, 2H), 4.95 (s, 4H), 2.41 (s, 6H), 1.68 (s, 6H).
BODIPY-2: ^{13}C NMR (126 MHz, DMSO-d_6) δ (ppm)
154.41, 150.68, 144.70, 143.23, 135.11, 130.92, 121.20, 101.48, 100.21, 14.63, 14.20.

Results and discussion

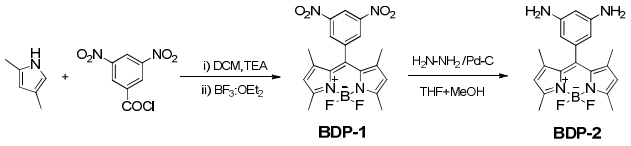

Scheme-1 Synthetic route of BODIPY probe.

For photophysical study absolute ethanol was the most suitable solvent among others. BODIPY-2 shows strong absorption peak in absolute ethanol at 499nm and very weak emission at 513nm. The weak emission is attributed to efficient fluorescence quenching resulting from photo induced electron transfer phenomenon. BODIPY having methyl groups at 1 and 7 position keeps the meso phenyl ring out of the plane of BODIPY core (fig.7a) and thus there is no conjugation between them but when this meso phenyl ring is substituted with amino group it impedes the emission. Amino group on angled meso phenyl ring contributes to the photoinduced electron transfer which suppresses the emission of the molecule. The engagement of electron density on amino group with other group could reset the emission is the idea behind construction of sensor. Two amino groups were placed on meso phenyl ring meta to each other with expectation of 1:2 binding stoichiometry with PA for better value of detection limit and binding constant. We have screened different nitro aromatics (10eq. each) i.e. picric acid(PA), p-nitrotoluene (PNT), 2,4-dinitrotoluene (DNT), 2,4,6-trinitrotoluene (TNT), p-nitrobenzioc acid (PNBA), p-nitrophenol (PNP), 2,4-dinitrophenol (DNP), 2,4,6-trichlorophenol (TCP), nitrobenzene (NBz) and keto RDX (kRDX) with 5 μM solution of BODIPY probe which shows high selectivity towards PA among others with 300 fold enhancement of fluorescence intensity and

quick response (with just gentle shaking in <10 seconds) in absolute ethanol. Fig.1 shows the graph for recognition of different NACs with BODIPY probe. The specificity of probe towards PA comes from the efficiency of association between them. Though electron withdrawing effect of nitro groups plays role in interactions the other NACs were insensitive to the probe.

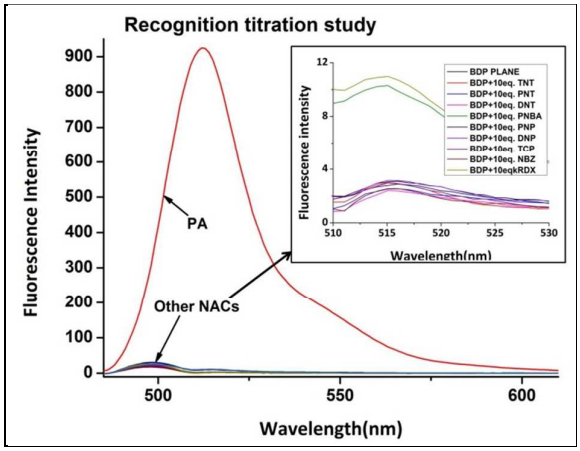

Fig.1 Fluorescence responses of BODIPY-2 (5 µM, λex= 499 nm) to the addition of various NACs (10 equiv.) Inset: Zoom view for recognition of different NACs.

The high selectivity of BODIPY probe to PA has been attributed to its specific binding with analyte because of proton transfer from PA to the amino group in sensor which is in accordance with static nature of association. This selectivity is further supported on the basis of pka values of NACs. PA has pka value =0.38 which is far less than its structurally resembled phenolic and nitroaromatic competitors such as DNP(4.11), PNP(7.15), PNBA(3.41), TCP(6.23) and TNT(11.99). Thus most acidic PA is preferred over all screened NACs. Excluding large enhancement in fluorescence intensity of BODIPY sensor with PA other signals were remain almost unaltered indicating its highest specificity towards PA. The interference of other NACs for PA sensing by sensor was studied by adding

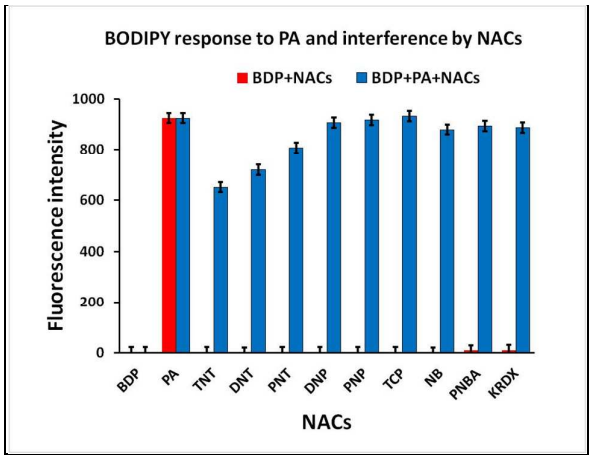

Fig.2 The histogram of fluorescence response of BODIPY-2 (5uM) to PA or other NACs (10 equiv. each, red bar) and to the mixture of other NACs (10 equiv.) with PA (10 equiv., blue bar) in absolute ethanol (with black error bar on top of each intensity bar).

different NACs (10 eq. each) in 5µM solution of BODIPY+ 10 eq.PA in ab. ethanol. This competitive binding experiment shows that there was no considerable lowering in fluorescence intensity by added NACs except PNT, DNT and TNT for which average 20% fall was observed. Fig. 2 shows the histogram of recognition and interference study. The binding constant derived from the fluorescence titration data in accordance with Benesi–Hildebrand plot was found to be Ka=1.91×10^{4}M^{-1} (Fig. 3) .

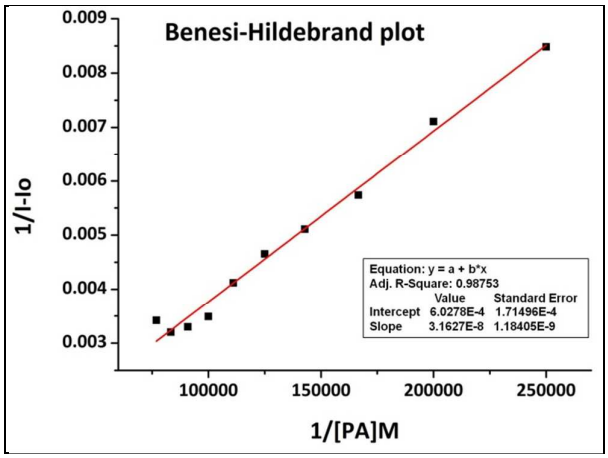

Fig.3 Benesi–Hildebrand plot of BODIPY-2 with PA in absolute. ethanol at λex = 499 nm. The binding constant (Ka) = 1.91x10^4 M^{-1}.

The sensitivity of BODIPY probe towards PA was counted on the scale of detection limit. From the changes in PA concentration dependent fluorescence intensity the detection limit was estimated to be 0.65ppb. For Benesi - Hildebrand plot and detection limit calculation fluorometric titration of BODIPY-2 with 1-12 equiv. PA was performed (Fig. S1, ESI). The Job's plot confirmed the 1:1 stoichiometry of the complexation between host and guest. The fluorescence intensity changes more rapidly when the concentration of PA increased from 0.5 to 1 equiv., implying a 1:1 complexation between BODIPY-2 and PA (Fig. 4).

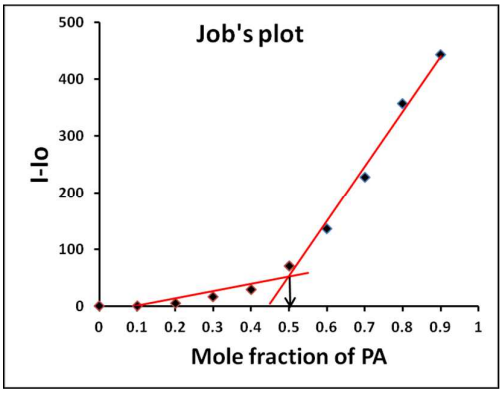

Fig.4 Job's plot of BODIPY probe with PA according to the of continuous variation method at λex = 499nm in ab.ethanol. [BODIPY-2] + [PA]=30μM.

It was expected to be 1:2 binding stoichiometry between probe and PA for larger value of binding constant as BODIPY has two amino groups on meso phenyl ring which can associate with two molecules of PA independently but it was 1:1. To have more understanding of the binding stoichiometry we have carried out ^{1}H NMR titration experiment. ^{1}H NMR spectrum of BODIPY-2 in

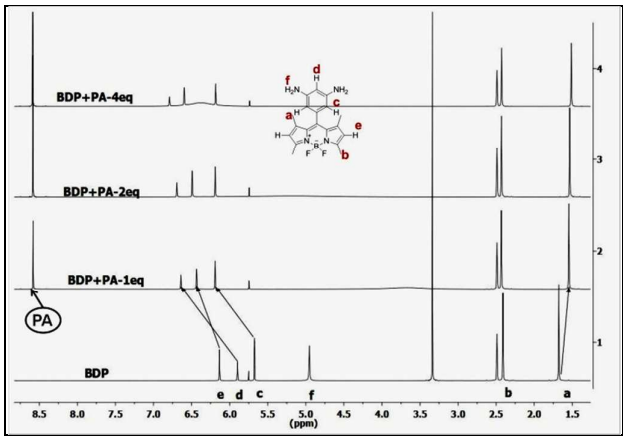

Fig.5 The stacked ^{1}H NMR titration spectra(500MHz) of BODIPY probe with 0, 1, 2 and 4 equivalent of PA in DMSO-d_6.

DMSO-d_6 was recorded with added 1, 2 and 4 equivalent of PA independently. Fig.5 shows the stacked graph of these titration experiments. After addition of 1 equivalent of PA to BODIPY-2 (1:1 stoichiometry) the peak **c** (for two symmetric protons on meso phenyl ring) and peak **e** (for 2 and 6 position protons on BODIPY core) shifted to deshielded region by 0.68ppm and 0.30ppm respectively. The another peak **d** (for proton between two amino groups on phenyl ring) comparatively get more shifted towards deshielded region by 0.74ppm as electron density from neighbouring amino group is engaged with added PA. The peak **f** (at 4.95 for amino protons) in plane BODIPY spectrum was vanished with added PA. Thus the aromatic region NMR signals were altered efficiently with added PA. When NMR spectrum was recorded with 2-equivalent of added PA (2:1 stoichiometry) the already altered signals by 1 equivalent PA were not shifted further considerably and same for added 4 equivalents also. This observation reveals that there was possibility of only 1:1 binding stoichiometry.

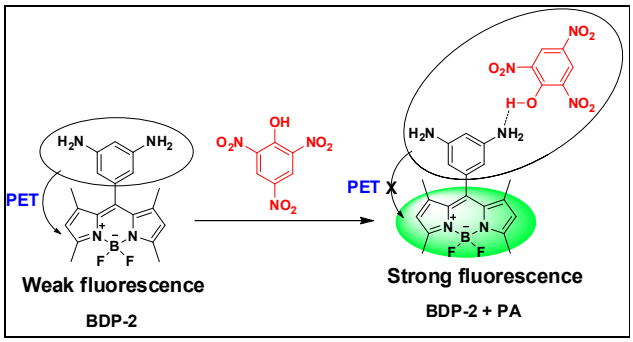

Fig.6 Proposed association pattern between BODIPY-2 and PA .

To get further insight into binding nature the DFT computation was carried out for BODIPY-2, BODIPY-2 + 1eq. PA and BODIPY-2 + 2eq. PA. Three structures were optimised at B3LYP/6-31g(d) level using Gaussian -09 software programme. Fig.7 shows the optimised Guass views of these structures respectively. Fig.7b shows the 1:1 binding in which one of the amino group on meso phenyl ring of BODIPY-2 get protonated from PA while picrate anion is stabilised by delocalisation of charge over tri nitro substituted ring . Fig.7c shows again 1:1 binding while second PA molecule become dissociated by the virtue of the molecular geometry.

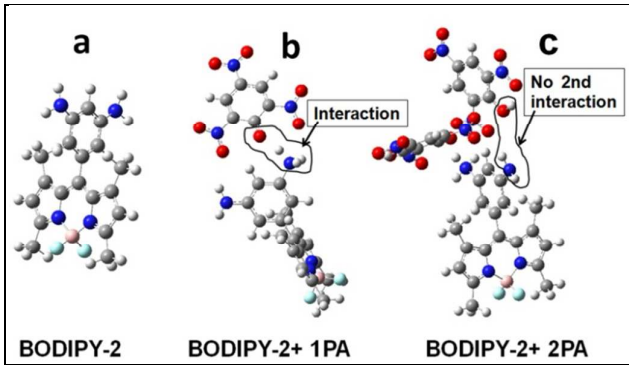

Fig.7 B3LYP/6-31g(d) Optimised structures with ball-stick model for BODIPY-2 and its association with 1 and 2 equivalent of PA. Ball colour – atom: gray-carbon, dark blue- nitrogen, pink-boron, red-oxygen, sky blue-fluorine, white-hydrogen.

In the light of Job's plot, ^{1}H NMR titration and DFT optimisation study it is confirmed that only 1:1 binding is possible between PA and BODIPY probe. The reason behind this might be explained by the fact that after protonation of one of the amino group with PA the meso diamine phenyl ring become electron deficient. This make it difficult the further association between the remaining amino group and the second PA molecule because of the molecular geometry constraint revealed by DFT optimisation. Isodensity plots of these optimised structures at B3LYP/6-31g(d) level shows that LUMO level of BODIPY-2 has some charge density on meso diamine phenyl ring which contributes to PET mechanism(Fig.S3,ESI). In case of both 1 and 2 equiv. PA associated structures there were no charge density on meso diaminophenyl ring at LUMO level which erases any possibility of assistance for PET process from meso position of BODIPY. Thus when one NH_2 group associates with PA

molecule it quaternises ($^{+}NH_3$) and makes the meso phenyl ring electron deficient so that lone pair of another NH_2 group is delocalised on phenyl ring more efficiently than in the case of unassociated BODIPY-2. Further electron density from the remaining free NH_2 and the phenyl ring is pulled by electron deficient complex of $^{+}NH_3$ and picrate anion. These things leave the still free NH_2 group with much less electron density compared to that in the unassociated BODIPY-2 and hence it neither binds with another PA molecule nor contributes to PET to limit the binding stoichiometry as 1:1. On the basis of acidic proton transfer from PA to probe the DFT and NMR study concludes that the association is of electrostatic nature which is further supported by salt screening effect study. The salt screening effect is a tool for determining electrostatic interaction between sensor and analyte[58].

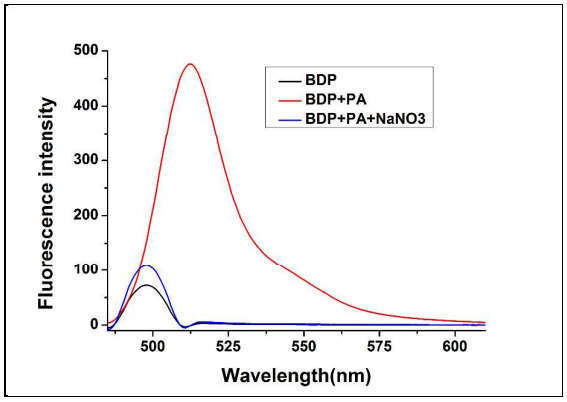

Fig.8 Salt screening effect study by interference of added $NaNO_3$ salt to PA sensing with BODIPY probe.

To study this effect the $NaNO_3$ salt with concentration (0.1M) more than PA(10μM) was added to the solution of BODIPY-2 probe (5μM) and PA (Fig.8). The result shows that after addition of $NaNO_3$ salt already enhanced fluorescence from sensor + PA mixture gets diminished to almost its original intensity of unbound sensor as added salt with higher concentration than PA eliminate the PA from vicinity of binding sites. This demonstrates the electrostatic association and proves why the probe is so sensitive and selective to PA over other NACs.

Conclusion:

We presented the simple meso diaminophenyl BODIPY probe for picric acid detection up to ppb level. This probe is highly selective towards picric acid and non sensitive to other equivalent NACs along with their least interference while sensing. Masking of PET process by picric acid through its association with parent non fluorescent BODIPY probe is effectively utilised for fluorescence enhancement signal. The binding mania is explained with different plots and supported by ^{1}H NMR and computational study. Thus less highlighted BODIPY and PET process in the field of picric acid sensing is bring in picture which could inspire further innovation in the area.

Acknowledgements:

One of the authors (Yogesh Erande) is thankful to University Grant Commission -SAP, India for financial support by way of Junior and Senior Research Fellowships.

References:

1 S. Singh, *J. Hazard. Mater.*, 2007, **144**, 15–28.

2 P. Cooper, *Wiley-VCH*, 1996, 33.

3 J. Akhavan, *R. Soc. Chem.*, 2004, **2nd edn**.

4 *John Wiley Sons New York*, 2000, **IIB**, 980.

5 E. H. Volwiler, *Ind. Eng. Chem.*, 1926, **18**, 1336–1337.

6 D. T. Meredith and C. O. Lee, *J. Am. Pharm. Assoc.*, 1939, **28**, 369.

7 C. Beyer, U. Böhme, C. Pietzsch and G. Roewer, *J. Organomet. Chem.*, 2002, **654**, 187–201.

8 V. Pimienta, R. Etchenique and T. Buhse, *J. Phys. Chem. A*, 2001, **105**, 10037–10044.

9 in *Resource of National Institutes of Health.*

10 J. Shen, J. Zhang, Y. Zuo, L. Wang, X. Sun, J. Li, W. Han and R. He, *J. Hazard. Mater.*, 2009, **163**, 1199–206.

11 Y. Salinas, R. Martínez-Máñez, M. D. Marcos, F. Sancenón, A. M. Costero, M. Parra and S. Gil, *Chem. Soc. Rev.*, 2012, **41**, 1261–96.

12 M. E. Germain and M. J. Knapp, *Chem. Soc. Rev.*, 2009, **38**, 2543–55.

13 Eric Wallis ; Todd M. Griffin ; Norm Popkie, Jr. ; Michael A. Eagan ; Robert F. McAtee, *Proc. SPIE*, 2005, **54**, 5795.

14 T. Q. Duong and J. S. Kim, *Chem. Rev.*, 2010, **110**, 6280–301.

15 R. Martínez-Máñez and F. Sancenón, *Chem. Rev.*, 2003, **103**, 4419–76.

16 S. J. Toal and W. C. Trogler, *J. Mater. Chem.*, 2006, **16**, 2871.

17 J.-S. Yang and T. M. Swager, *J. Am. Chem. Soc.*, 1998, **120**, 11864–11873.

18 S. S. Nagarkar, B. Joarder, A. K. Chaudhari, S. Mukherjee and S. K. Ghosh, *Angew. Chemie Int. Ed.*, 2013, **52**, 2881–2885.

19 Y. Wang and Y. Ni, *Anal. Chem.*, 2014, **86**, 7463–70.

20 V. Béreau, C. Duhayon and J.-P. Sutter, *Chem. Commun. (Camb).*, 2014, **50**, 12061–4.

21 B. Liu, C. Tong, L. Feng, C. Wang, Y. He and C. Lü, *Chemistry*, 2014, **20**, 2132–7.

22 N. Venkatramaiah, D. M. G. C. Rocha, P. Srikanth, F. A. Almeida Paz and J. P. C. Tomé, *J. Mater. Chem. C*, 2015, **3**, 1056–1067.

23 A. Narayanan, O. P. Varnavski, T. M. Swager and T. Goodson, *J. Phys. Chem. C*, 2008, **112**, 881–884.

24 X.-G. Li, Y. Liao, M.-R. Huang, V. Strong and R. B. Kaner, *Chem. Sci.*, 2013, **4**, 1970.

25 M. S. Meaney and V. L. McGuffin, *Anal. Chim. Acta*, 2008, **610**, 57–67.

26 K. Zhang, H. Zhou, Q. Mei, S. Wang, G. Guan, R. Liu, J. Zhang and Z. Zhang, *J. Am. Chem. Soc.*, 2011, **133**, 8424–7.

27 J.-D. Xiao, L.-G. Qiu, F. Ke, Y.-P. Yuan, G.-S. Xu, Y.-M. Wang and X. Jiang, *J. Mater. Chem. A*, 2013, **1**, 8745.

28 B. Roy, A. K. Bar, B. Gole and P. S. Mukherjee, *J. Org. Chem.*, 2013, **78**, 1306–10.

29 S. Kumar, N. Venkatramaiah and S. Patil, *J. Phys. Chem. C*, 2013, **117**, 7236–7245.

30 P. Vishnoi, S. Sen, G. N. Patwari and R. Murugavel, *New J. Chem.*, 2015, **39**, 886–892.

31 K. D. Prasad and T. N. Guru Row, *RSC Adv.*, 2014, **4**, 45306–45310.

32 G. Sivaraman, B. Vidya and D. Chellappa, *RSC Adv.*, 2014, **4**, 30828.

33 A. Yadav and R. Boomishankar, *RSC Adv.*, 2015, **5**, 3903–3907.

34 R. Chopra, V. Bhalla, M. Kumar and S. Kaur, *RSC Adv.*, 2015, **5**, 24336–24341.

35 W. C. T. Jason C. Sancheza, *J. Mater. Chem.*, 2008, **18**, 3143–3156.

36 S. S. and Y. P. Yongqian Xu, Benhao Li, Weiwei Li, Jie Zhao, *Chem. Commun.*, 2013, **49**, 4764–4766.

37 S. Sandhu, R. Kumar, P. Singh, A. Mahajan, M. Kaur and S. Kumar, *ACS Appl. Mater. Interfaces*, 2015, **7**, 10491–10500.

38 A. Gupta, Y.-A. Kang, M.-S. Choi and J. S. Park, *Sensors Actuators B Chem.*, 2015, **209**, 225–229.

39 N. Venkatramaiah, D. M. G. C. Rocha, P. Srikanth, F. a. Almeida Paz and J. P. C. Tomé, *J. Mater. Chem. C*, 2015, **3**, 1056–1067.

40 A. Chowdhury and P. S. Mukherjee, *J. Org. Chem.*, 2015, **80**, 4064–4075.

41 A. U. Palma-Cando and U. Scherf, *ACS Appl. Mater. Interfaces*, 2015, 150506112911002.

42 O. Pinrat, K. Boonkitpatarakul, W. Paisuwan, M. Sukwattanasinitt and A. Ajavakom, *Analyst*, 2015, **140**, 1886–1893.

43 C. Zhang, L. Sun, Y. Yan, J. Li, X. Song, Y. Liu and Z. Liang, *Dalt. Trans.*, 2015, **44**, 230–236.

44 K. Acharyya and P. S. Mukherjee, *Chem. Commun.*, 2014, **50**, 15788–15791.

45 N. Boens, V. Leen and W. Dehaen, *Chem. Soc. Rev.*, 2012, **41**, 1130–72.

46 A. Loudet and K. Burgess, *Chem. Rev.*, 2007, **107**, 4891–932.

47 O. Buyukcakir, O. A. Bozdemir, S. Kolemen, S. Erbas and E. U. Akkaya, *Org. Lett.*, 2009, **11**, 4644–7.

48 J.-H. Olivier, A. Haefele, P. Retailleau and R. Ziessel, *Org. Lett.*, 2010, **12**, 408–11.

49 H. He, P.-C. Lo, S.-L. Yeung, W.-P. Fong and D. K. P. Ng, *Chem. Commun. (Camb).*, 2011, **47**, 4748–50.

50 A. B. Nepomnyashchii, S. Cho, P. J. Rossky and A. J. Bard, *J. Am. Chem. Soc.*, 2010, **132**, 17550–9.

51 A. Ding, L. Yang, Y. Zhang, G. Zhang, L. Kong, X. Zhang, Y. Tian, X. Tao and J. Yang, *Chemistry*, 2014, **20**, 12215–22.

52 R. M. Frisch MJ, Trucks GW, Schlegel HB, Scuseria GE, P. G. Cheeseman JR, Scalmani G, Barone V, Mennucci B, B. J. Nakatsuji H, Caricato M, Li X, Hratchian HP, Izmaylov AF, F. R. Zheng G, Sonnenberg JL, Hada M, Ehara M, Toyota K and F. D. Hasegaw CJ, 2010.

53 O. Treutler and R. Ahlrichs, *J. Chem. Phys.*, 1995, **102**, 346.

54 A. D. Becke, *J. Chem. Phys.*, 1993, **98**, 5648.

55 C. Lee, W. Yang and R. G. Parr, *Phys. Rev. B*, 1988, **37**, 785–789.

56 E. V. Antina, G. B. Guseva, A. E. Loginova, A. S. Semeikin and A. I. V'yugin, *Russ. J. Gen. Chem.*, 2010, **80**, 2374–2381.

57 Q. Li, J. Xu, Y. Yue, Y. Liao and S. Shao, *Anal. Methods*, 2014, **6**, 6531.

58 G. He, H. Peng, T. Liu, M. Yang, Y. Zhang and Y. Fang, *J. Mater. Chem.*, 2009, **19**, 7347.